Broadband Mid-Infrared Supercontinuum Spectra Spanning 2–15 μm Using As2Se3 Chalcogenide Glass Triangular-Core Graded-Index Photonic Crystal Fiber

Article *in* Journal of Lightwave Technology · September 2015

DOI: 10.1109/JLT.2015.2418993

CITATIONS
100

READS
823

3 authors:

Than Singh Saini
National Institute of Technology, Kurukshetra
125 PUBLICATIONS **928** CITATIONS
SEE PROFILE

Ajeet Kumar
Delhi Technological University
116 PUBLICATIONS **825** CITATIONS
SEE PROFILE

Ravindra Sinha
Delhi Technological University
431 PUBLICATIONS **3,449** CITATIONS
SEE PROFILE

Broadband Mid-Infrared Supercontinuum Spectra Spanning 2–15 μm Using As_2Se_3 Chalcogenide Glass Triangular-Core Graded-Index Photonic Crystal Fiber

Than Singh Saini, *Member, IEEE, Member, OSA*, Ajeet Kumar, *Member, IEEE, Member, OSA*, and Ravindra Kumar Sinha, *Member, IEEE, Member, OSA*

***Abstract*—In this paper, we report analysis, design, and numerical modeling of mid-infrared supercontinuum generation across 2–15 μm molecular "fingerprint region" using a new design of triangular-core graded-index photonic crystal fiber (PCF) pumped with 50 fs laser pulses of peak power of 3.5 kW at 4.1 μm. Proposed PCF design offers the nonlinear coefficient as high as 1944 $W^{-1} \cdot Km^{-1}$ at pump wavelength. To the best of our knowledge, the supercontinuum in PCF with such broadband spectra has been reported first time. Proposed PCF design has potential applications in gas sensing, food quality control, and early cancer diagnostics.**

***Index Terms*—Highly nonlinear photonic crystal fiber, mid-infrared supercontinuum, nonlinear optics.**

I. Introduction

DURING the last decade white-light supercontinuum generation (SCG) in optical fibers has emerged as an active and exciting research field. Various types of new light sources have been created which are finding applications in a diverse range of fields such as optical coherence tomography [1], [2], optical communications [3], frequency metrology [4], fluorescence lifetime imaging [5], gas sensing [6], [7], food quality control [8] and early cancer diagnostics [9]. Supercontinuum (SC) is formed when a large number of nonlinear processes such as self phase modulation (SPM), stimulated Raman scattering, cross-phase modulation and four-wave mixing act together upon a pump beam in order to cause extensive spectral broadening of the original pump beam. The breakthroughs in recent years have raised scientific concerns to understand and model how all these nonlinear processes interact together to generate SC and how parameters can be engineered to control and enhance the SC spectra.

The mid-infrared region is important because the fundamental molecular vibration absorption bands are stronger than the overtones and combination vibration absorption bands situated in the near-infrared region. Mid-infrared spectroscopy is able to provide thorough understanding of the molecular structure of matter and to perform non-intrusive diagnostics of composite systems of physical, chemical and biological interest. SC spectra spanning visible to near-infrared in silica based fibers have been generated previously for various applications [10]–[12]. However, the broadening of SC spectra in silica fibers is limited by the strong material absorption beyond 2.5 μm wavelength, which effectively limits the spectral evolution into the mid-infrared region. For this reason a large number of non-silica glasses such as tellurite, ZBLAN, bismuth, fluoride and chalcogenide have been proposed for SCG in mid-infrared region [13]–[19].

Among all non-silica glasses, the chalcogenide glasses are excellent candidates for mid-infrared region because some of its compositions possess optical transparency upto 25 μm in this region [20]. The As_2Se_3 glass has shown excellent optical transparency between 0.85–17.5 μm with attenuation coefficient of less than 1 cm^{-1} [20]. In addition to broadband mid-infrared transmission window, chalcogenide glasses have also very large linear and nonlinear refractive indices which make them promising candidates for mid-infrared SCG [21]. Shaw *et al.* [22] presented an experimental demonstration of SCG in the spectral range from 2.1 to 3.2 μm using hexagonal structure of As_2Se_3 based chalcogenide photonic crystal fiber (PCF). Recently, Hu *et al*. [23] gave a design procedure, which can be used to maximize the band-width of SCG in As_2Se_3 chalcogenide PCFs, for more than 4 μm band-width of SC. Kubat *et al.* [24] presented a numerical design optimization of ZBLAN fibers for mid-infrared SC sources using direct pumping with 10 ps pulses from mode-locked Yb and Er lasers to obtain broad spectra ranging from 1 to 4.5 μm. Klimczak *et al.* [25] achieved SC broadening between 930 to 2170 nm spectral range using all-solid soft glass microstructured optical fiber. Kubat *et al.* Ref. [26] have experimentally demonstrated the SCG covering 0.9–9 μm with the help of commercially available ZBLAN fiber and commercially available chalcogenide PCF. Recently, Kubat *et al.* [27] presented numerical modelling of broadband mid-infrared SCG spanning from 3–12.5 μm in step-index fiber pumped at 4.5 μm with 0.75 kW pump power. Petersen *et al.* [28] demonstrated broadband mid-infrared SC spectra covering the

Manuscript received December 30, 2014; revised March 17, 2015 and March 30, 2015; accepted March 30, 2015. Date of publication March 31, 2015; date of current version August 9, 2015. This work was supported by the "TIFAC-Center of Relevance and Excellence" in Fiber Optics and Optical Communication at Delhi Technological University (Formerly Delhi College of Engineering) Delhi, through the "Mission REACH" program of Technology Vision-2020 of the Government of India and by the TUN-IND Bilateral Research Project "Design, modeling and characterization of highly nonlinear fibers for all-optical high bit-rate network," supported by the Ministry of Higher Education and Scientific Research of the Republic of Tunisia and the Department of Science and Technology, Government of India.

The authors are with the Technology Information, Forecasting and Assessment Council, Center of Relevance and Excellence in Fiber Optics and Optical Communication, Department of Applied Physics, Delhi Technological University, Delhi 110042, India (e-mail: tsinghdph@gmail.com; ajeetdph@gmail.com; dr_rk_sinha@yahoo.com).

Color versions of one or more of the figures in this paper are available online at http://ieeexplore.ieee.org.

Digital Object Identifier 10.1109/JLT.2015.2418993

range of 1.4–13.3 μm in mid-infrared regime using ultra-high NA chalcogenide step-index fiber.

In comparison to SCG in standard optical fibers, PCF requires input laser pulses with very less initial peak power. The higher order dispersion effects are stronger in PCF and play a much more significant role in pulse propagation. The dramatic spectral broadening with relatively low-intensity laser pulses in PCF is very interesting phenomena and can be used in various fascinating applications such as frequency metrology.

The broadening mechanism of SC spectrum mainly depends upon the dispersion profile of optical fiber structure as well as input pulse characteristics. In the anomalous group velocity dispersion (GVD) regime when highly intense laser pulse incident on nonlinear medium it evolves towards the higher-order solitons [29]. For the femtosecond pumping, the higher-order solitons are affected by the higher-order dispersion and stimulated Raman scattering. Consequently, the higher order solitons become unstable and breakup into several fundamental solitons through the fission process. Such chaotic soliton fission process causes shot-to-shot noise in the SC spectrum [30], [31]. But in case of normal GVD regime, for femtosecond pulses SPM is the only reason for ultra wide spectral broadening [31]. This makes such broad-band SC suitable for time-resolved applications such as optical coherence tomography, pump-probe spectroscopy and nonlinear microscopy. One of the possibilities for generating SC in the normal dispersion regime is to pump the fiber far below the zero dispersion wavelength, so that the generated spectrum does not extend into the anomalous dispersion region. However, this would require high power or very short pulses to overcome the short effective interaction length due to high value of dispersion. It is worthwhile to mention here that the broadening of SC demonstrated in [28] is the largest achieved in fiber geometry till date. However, possibility of broadening of SC spectra beyond 20 μm is being discussed in scientific news and views [32].

Mid-infrared domain in the range of 2–15 μm of electromagnetic spectrum is of particular importance because of the molecular fingerprint of biological tissue lie within this domain. This domain is useful to determine a tissue spectral map which provides very important information about the existence of diseases such as cancer. Therefore, it is necessary to develop broadband SC sources in mid-infrared domain. The chalcogenide glasses have this potential to provide such broadband mid-infrared SC sources.

In this paper we present analysis, design and numerical modeling for achieving ultra broadband mid-infrared SC spectra spanning 2–15 μm using As_2Se_3 based chalcogenide-glass triangular-core graded-index (TCGI) PCF. To obtain efficient broadband SC spectrum in mid-infrared regime, proposed TCGI PCF has been specifically designed for all-normal dispersion characteristic. Such broadband mid-infrared SC spectrum is obtained in relatively short length (i.e., 5 mm) of PCF, using a sub-harmonic generation source of the mode-locked thulium 50 fs pulsed fiber laser at 4.1 μm [33].

This paper is organized in five sections. Section I provides a brief introduction and overview of previous works on SCG in PCFs. In Section II, detailed description of method of analysis is given. Section III explains the design of proposed TCGI PCF. Section IV is devoted to the results and discussion. Finally, conclusion of this work is summarized in Section V.

II. Method of Analysis

A. Linear Characteristics of PCF Structure

To simulate the effective index of fundamental mode propagating through proposed TCGI PCF, a full vectorial finite element method based software "COMSOL Multiphysics" has been employed. For calculating the wavelength dependent refractive index of As_2Se_3 based chalcogenide material following two terms Sellmeier equation has been used [34]

$$n^2 - 1 = A_0 + \sum_{n=1}^{2} \frac{A_n \lambda^2}{\lambda^2 - a_n^2}. \tag{1}$$

In above Eq. (1) A_0, A_n and a_n are the sellmeier coefficients with $A_0 = 3.3344$, $a_1 = 0.43834$ μm, $a_2 = 41.395$ μm, $A_1 = 3.3105$ and $A_2 = 0.89672$ for As_2Se_3 based chalcogenide glass which we have used as a fiber material in this work.

The GVD plays an important role in SCG because it determines the extent to which different spectral components of an ultra-short pulse propagate at different phase velocities in the PCF. The GVD, $D(\lambda)$ is calculate from wavelength dependent effective indices of propagating mode using the following relation [29]

$$D(\lambda) = -\frac{\lambda}{c} \frac{\partial^2 \mathrm{Re}(n_{\mathrm{eff}})}{\partial \lambda^2} \tag{2}$$

where c is the velocity of light in free space, $\mathrm{Re}(n_{\mathrm{eff}})$ is the real part of the effective index. Both material and waveguide dispersion are included in the above equation as Sellmeier equation is taken into account while calculating n_{eff}.

The effective area of propagating mode in the PCF is calculated using the relation given below [27], [29]

$$A_{\mathrm{eff}} = \frac{\left(\int \int_{-\infty}^{\infty} |E|^2 \, dxdy \right)^2}{\left(\int \int_{-\infty}^{\infty} |E|^4 \, dxdy \right)} \tag{3}$$

where E is the electric field distribution derived by solving the eigenvalue problem drawn from Maxwell's equations.

B. Nonlinear Characteristics of PCF Structure

Nonlinearity in PCF is the most important parameter which must be studied more rigorously in order to get accurate results. The nonlinear coefficient (γ), offered by PCF structure, related to the nonlinear refractive index of material of PCF and the effective area of propagating mode as follows [29]:

$$\gamma = \frac{2\pi n_2}{\lambda A_{\mathrm{eff}}(\lambda)} \tag{4}$$

where n_2 is the nonlinear refractive index of material ($n_2 = 5.2 \times 10^{-18}$ m^2/W at 4.5 μm wavelength [27]), λ is the pump wavelength and A_{eff} is the effective area of fundamental mode and its value depends on the wavelength. For broader SC spectra the nonlinear refractive index (i.e., n_2) should be as high as possible and A_{eff} should be as small as possible. Wavelength

dependent effective mode area is obtained using Eq. (3) as mentioned in Ref. [27]. The value of γ can be enhanced by taking material with high non linear refractive index and/or by designing a PCF with lower effective mode area.

To simulate SC, the following generalized nonlinear Schrodinger equation has been solved for output pulse envelope, *A* (*z*, *t*) using split-step Fourier method [10]

$$\frac{\partial A}{\partial z} + \frac{\alpha}{2}A - \left(\sum_{n\geq 2}\beta_n \frac{i^{n+1}}{n!}\frac{\partial^n A}{\partial t^n}\right) = i\gamma\left(1+\frac{i}{\omega_o}\frac{\partial}{\partial t}\right)\left[A(z,t)\int_{-\infty}^{\infty} R(t')\left|A(z,t-t')\right|^2 dt'\right]. \quad (5)$$

The left hand side of Eq. (5) deals with linear propagation effects while the right hand side of this deals with nonlinear effects of PCF structure. α represents the power losses in the PCF as the light travels through it. We have included both the material and confinement losses in all the simulations. A constant material loss coefficient of 0.6 cm^{-1} has been considered for 2–15 μm spectral range [20]. For designed TCGI PCF the typical value of simulated confinement loss is $\sim 3.9 \times 10^{-5}$ dB/mm at 4.1 μm. The propagation constant (β) at any frequency (ω), relative to pulse central frequency (ω_0) , can be expanded as Taylor series expansion [10]

$$\beta(\omega) = \beta(\omega_0) + \beta_1(\omega_0)(\omega-\omega_0) + \frac{1}{2!}\beta_2(\omega_0)(\omega-\omega_0)^2 + \frac{1}{3!}\beta_2(\omega_0)(\omega-\omega_0)^3 + \cdots \quad (6)$$

where $\beta_n(\omega_0) = \dfrac{d^n\beta}{d\omega^n}$, first term in the right hand side of Eq. (6) gives the effective refractive index of the propagating mode and the second and third terms are related to the group velocity and the GVD of the pulse respectively. We have evaluated higher order dispersion up to the order of 9th from the GVD curve.

R (t′) is the nonlinear response function and takes account of the electronic and nuclear contributions and expressed as follows:

$$R(t') = (1-f_R)\,\delta(t'-t_e) + f_R h_R(t') \quad (7)$$

where f_R is the fractional contribution of the Raman response to the total linear response. For As_2Se_3 chalcogenide glasses the fractional contribution $f_R = 0.115$ [35]. The electronic contribution is treated in this analysis as occurring instantaneously because $t_e \approx 1$ fs. h_R *(t′)* is the Raman response function and contains information on the vibration of material molecules as light passes through the fiber.

The Raman response function h_R *(t′)* can be calculated by most common and approximate analytic form which is given by the following relation:

$$h_R(t') = \frac{\tau_1^2+\tau_2^2}{\tau_1\tau_2}\exp\left(-\frac{t'}{\tau_2}\right)\sin\left(\frac{t'}{\tau_1}\right) \quad (8)$$

where Raman period $\tau_1 = 23.1$ fs and life time $\tau_2 = 195$ fs for As_2Se_3 based glasses [35].

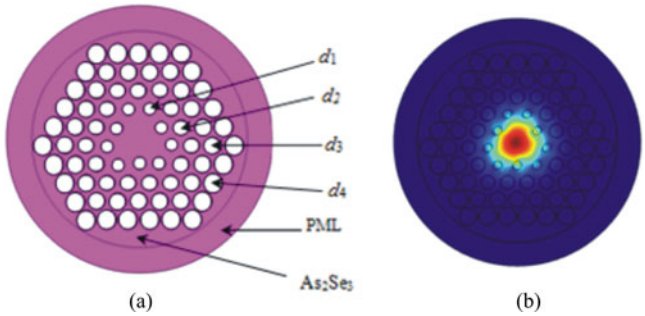

Fig. 1. (a) Transverse cross-section of proposed TCGI PCF; (b) the electric field distribution of propagating mode in PCF at 4.1 μm.

In our study, we consider the hyperbolic secant pulse as input pulse which is expressed as the relation given below:

$$A(z=0,t) = \sqrt{P_0}\cdot \operatorname{sech}\left(\frac{t}{t_o}\right) \quad (9)$$

where $t_0 = T_{\text{FWHM}}/1.7627$ and P_0 is peak power of input pulse.

III. Design of Proposed TCGI PCF

We present a novel TCGI PCF structure with four layers of air holes arranged in triangular lattice pattern in As_2Se_3-based chalcogenide glass. As shown in Fig. 1(a) three air holes have been removed from the centre to construct a triangular-core of the PCF. The center to center distance of air holes is taken as constant and represented byΛ. The diameters of air holes in first, second, third and fourth ring are d_1, d_2, d_3 and d_4 respectively. For our design $d_1 < d_2 < d_3 < d_4$, i.e., the air filling fraction (d_n/Λ, $n = 1, 2, 3, 4$) of cladding increases with "*n*", where "*n*" is the number of rings of air holes. In other words the effective refractive index of cladding successively decreases for first, second, third and fourth rings of air holes. That is why the structure of PCF is named as "graded-index". The structure is surrounded by the cylindrical perfectly matched layer (PML) for eliminating the back reflection effect at the boundary. The reason of designing TCGI PCF is to get all-normal and nearly zero dispersion characteristic at desired pump wavelength. Triangular shaped core and Graded index profile of air holes increase the confinement of field and thus increase the nonlinearity. Gradually increasing shape of air holes effectively generates an equivalent refractive index profile of monotonically decreasing refractive index. Such a design is having strong control in achieving the ultra broadband flatted dispersion [36] which is essential for achieving ultra broadband SCG. Simulated electric field distribution of propagating mode in proposed TCGI PCF at 4.1 μm has been illustrated in Fig. 1(*b*).

IV. Results and Discussion

In order to obtain ultra broadband SC in proposed PCF structure, we have optimized the structural parameters (i.e., Λ, d_1, d_2, d_3 and d_4) to achieve all-normal chromatic dispersion profile. The effect of various values of air hole diameter in first

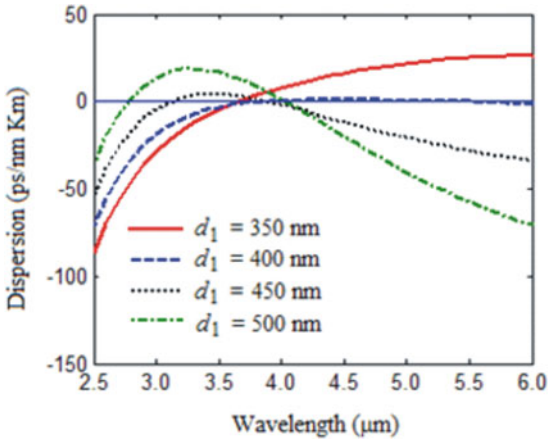

Fig. 2. The effect of the diameter of the air holes in first ring (i.e., d_1) on chromatic dispersion profile while keeping other parameters fixed as: $d_2 = 700$ nm, $d_3 = 800$ nm, $d_4 = 900$ nm, and $\Lambda = 1000$ nm.

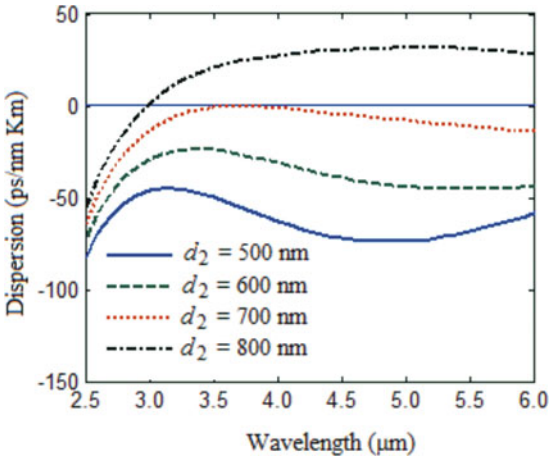

Fig. 3. The effect of the diameter of the air holes in second ring (i.e., d_2) on chromatic dispersion profile while keeping other parameters fixed as: $d_1 = 420$ nm, $d_3 = 800$ nm, $d_4 = 900$ nm, and $\Lambda = 1000$ nm.

TABLE I
GEOMETRICAL PARAMETERS OF PROPOSED TCGI PCF

Parameter name	Pitch	d_1	d_2	d_3	d_4
Parameter value	1000 nm	420 nm	700 nm	800 nm	900 nm

ring, d_1 on dispersion characteristic, while keeping other parameters fixed, is illustrated in Fig. 2. Similarly the effect of diameter of air holes in second ring on the dispersion profile of proposed triangular-core PCF is shown in Fig. 3. It is to be noted here that we have simulated the effect of the diameters of air holes in third and fourth ring and found that they are relatively less sensitive on dispersion characteristic of proposed PCF structure (not shown in figure). For optimized geometrical parameters (as shown in Table I), the chromatic dispersion profile of proposed TCGI PCF is shown in Fig. 4. The proposed PCF structure offers flat dispersion across 3.35–4.20 μm spectral range within the dispersion value of approximately –2 ps/(nm $\times$ Km). Confinement loss is

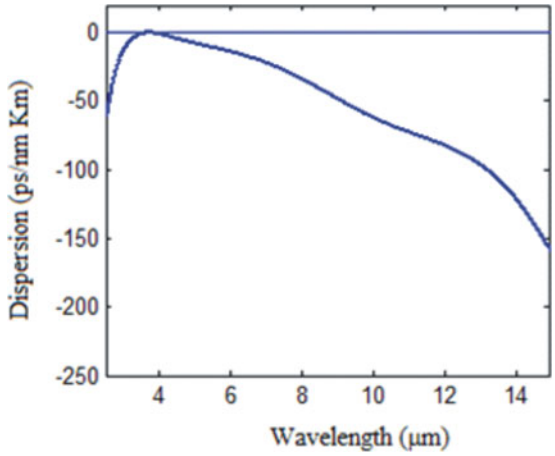

Fig. 4. The chromatic dispersion characteristic of proposed TCGI PCF structure with optimized parameters (i.e., $d_1 = 420$ nm, $d_2 = 700$, $d_3 = 800$ nm, $d_4 = 900$ nm, and $\Lambda = 1000$ nm).

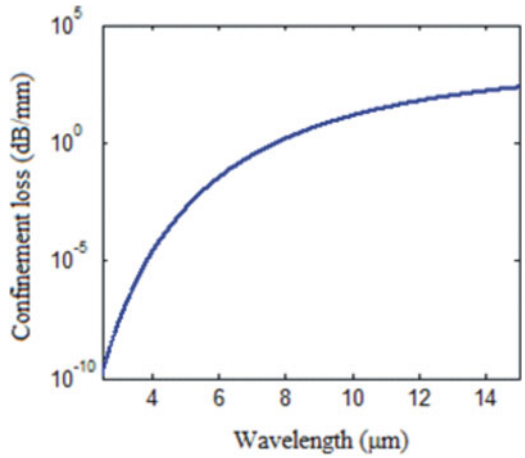

Fig. 5. The confinement loss of proposed TCGI PCF structure with optimized parameters (i.e., $d_1 = 420$ nm, $d_2 = 700$, $d_3 = 800$ nm, $d_4 = 900$ nm, and $\Lambda = 1000$ nm).

very improtant parameter for generating SC spectra in fibers. We have simulated the confinement loss of our proposed PCF structure and shown in Fig. 5. Proposed PCF structure offers low confinement loss of $\sim 3.9 \times 10^{-5}$ dB/mm at pump wavelength (i.e., 4.1 μm). However, the loss at 10 μm is $\sim$14 dB/mm. Since the higher wavelengths ($>$8 μm) generate at 5 mm length of the PCF, the broadening of supercontinumm spectrum would not be affected by higher losses at higher wavelengths.

The wavelength dependent effective-mode-area of propagating mode and corresponding nonlinear coefficient has been illustrated in Fig. 6. Simulated results show that the proposed TCGI PCF structure offers nonlinear coefficient (γ) as high as 1944 $W^{-1} \cdot Km^{-1}$ with effective mode area of 4.1 μm^2 at 4.1 μm input pump wavelength.

As illustrated in Fig. 7, by launching the laser pulses of proper parameters (pulse parameters are shown in Table II) we are able to obtain broadband spectra ranging 2–15 μm in only 5 mm length of proposed TCGI PCF. The

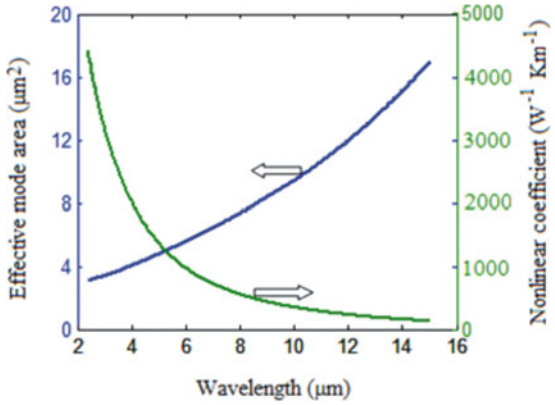

Fig. 6. The variation of effective mode area of propagating mode and corresponding nonlinear coefficient of proposed TCGI PCF with optimized parameters (i.e., $d_1 = 420$ nm, $d_2 = 700$, $d_3 = 800$ nm, $d_4 = 900$ nm, and $\Lambda = 1000$ nm).

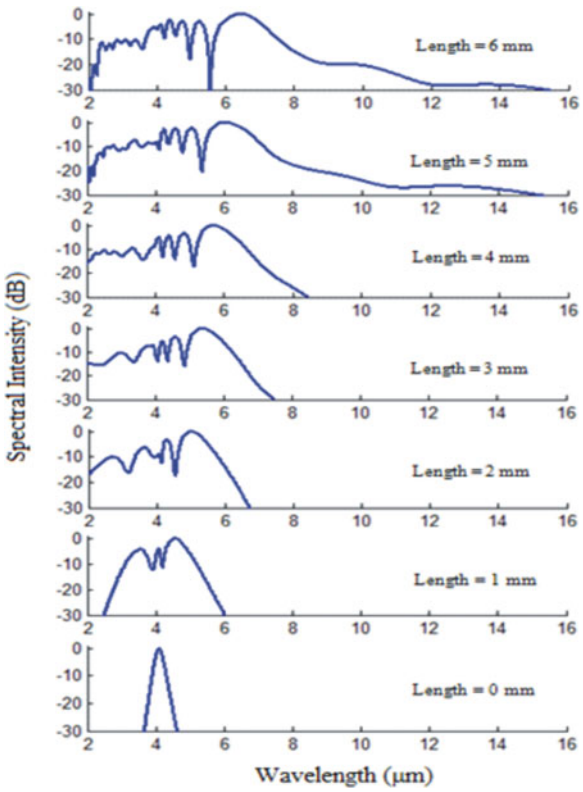

Fig. 7. Spectral broadening of SC spectra from various length of PCF; when 50 fs laser pulses with peak power of 3.5 kW launched at proposed TCGI PCF structure.

TABLE II
OPTIMIZED INPUT PULSE PARAMETERS

Parameter name	Peak power	T_{FWHM}	Pulse shape
Parameter value	3.5 kW	50 fs	hyperbolic secant

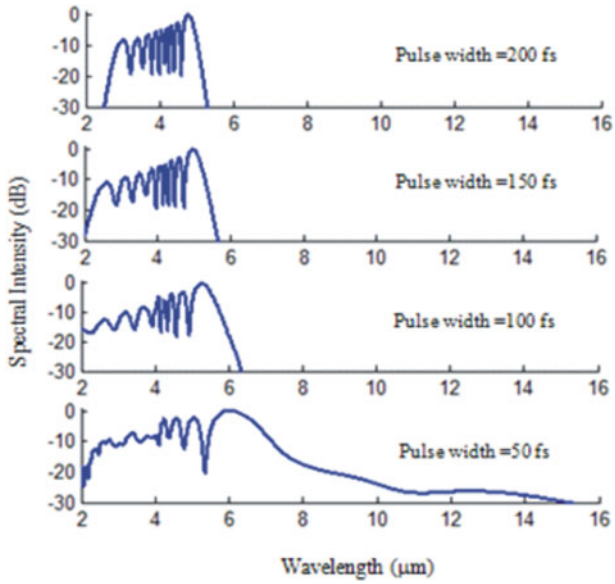

Fig. 8: Broadening of output spectra from 5 mm long TCGI PCF obtained at various values of pulse width (T_{FWHM}) when peak power of incident pulses = 3.5 kW.

calculated values of nonlinear length ($L_{\mathrm{NL}} = 1/\gamma P_0$) and dispersion length ($L_D = \dfrac{T_0^2}{\beta_2}; T_0 = T_{\mathrm{FWHM}}/1.763$), for proposed PCF are 1.47×10^{-4} m and 5.2×10^{-2} m respectively for 50 fs laser pulse at 4.1 μm. The solitons order, $N \approx \sqrt{\mathrm{L_D}/\mathrm{L_{NL}}}$ is 18 for proposed PCF structure. The solitons fission length, $L_{\mathrm{fiss}} = L_D/N$ is equal to 2.76 mm. Within 5 mm length of the TCGI PCF an ultra-broadband SC extending from 2–15 μm has been generated with 50 fs laser pulses of peak power of 3.5 kW. As shown in Fig. 7, beyond 5 mm length of the PCF the broadening of SC spectra does not increase significantly. This is because of the lower nonlinearity and higher losses at wavelengths greater than 15 μm for proposed TCGI PCF structure.

Finally, the influence of the input pulse width, i.e., full width at half maximum (T_{FWHM}) on the bandwidth of output spectrum in 5 mm long TCGI PCF has been revealed in Fig. 8. The input peak power is fixed at 3.5 kW. When the value of T_{FWHM} increases the output spectra start to get narrower. This is due to the SPM effect. It is to be noted here that the short pulse is better to get broader SC spectra. The optimized values of input pulse are summarized in Table II.

Proposed TCGI PCF structure can be fabricated by standard extrusion and stacking based methods. For fabrication purposes it is also very important to investigate the tolerance of the proposed structure with respect to the various design parameters. After investigating the effect of small variations in the values of d_1, d_2, d_3, d_4 and Λ we have found that the magnitude of dispersion and the effective mode area of propagating mode are less sensitive to the structural parameters. For example, at 4.1 μm wavelength 1% variation in d_1 changes the dispersion value by $\sim$ 4% and changes the effective mode area by 0.8%. These changes produce only $\sim$1% changes in the spectral broadening of SC spectra.

V. Conclusion

A new design of TCGI PCF for ultra-broadband SCG in mid-infrared regime covering atmospheric transparent windows (i.e., 3–5 μm, and 8–13 μm of spectrum region) and the molecular "fingerprint region" from 2–15 μm, is reported in this paper. Such broadband mid-infrared spectrum is achieved by launching 50 fs laser pulses from mode-locked Tm-doped fiber laser with peak power of 3.5 kW on a very small length (i.e., 5 mm) of proposed PCF. Simulated results indicate that the proposed PCF structure offers nonlinear coefficient as high as 1944 $W^{-1} \cdot Km^{-1}$ at 4.1 μm pump wavelength with effective mode area of 4.1 μm^2. This new type of PCF can be a good candidate for generating efficient SC which is applicable for various nonlinear applications such as gas sensing, food quality control and early cancer diagnostics.

References

[1] I. Hartl, X. D. Li, C. Chudoba, R. K. Ghanta, T. H. Ko, J. G. Fujimoto, J. K. Ranka, and R. S. Windeler, "Ultrahigh-resolution optical coherence tomography using continuum generation in an air-silica microstructure optical fiber," *Opt. Lett.*, vol. 26, pp. 608–610, 2001.

[2] P. Hsiung, Y. Chen, T. H. Ko, J. G. Fujimoto, C. J. S. De Matos, S. V. Popov, J. R. Taylor, and V. P. Gapontsev, "Optical coherence tomography using a continuous-wave, high-power, Raman continuum light source," *Opt. Exp.*, vol. 12, pp. 5287–5295, 2004.

[3] H. Takara, T. Ohara, T. Yamamoto, H. Masuda, M. Abe, H. Takahashi, and T. Morioka, "Field demonstration of over 1000-channel DWDM transmission with supercontinuum multi-carrier source," *Electr. Lett.*, vol. 41, pp. 270–271, 2005.

[4] J. Ye, H. Schnatz, and L. Hollberg, "Optical frequency combs: From frequency metrology to optical phase control," *IEEE J. Sel. Topics Quantum Electron.*, vol. 9, no. 4, pp. 1041–1058, Jul./Aug. 2003.

[5] C. Dunsby, P. M. P. Lanigan, J. McGinty, D. S. Elson, J. Requejo-Isidro, I. Munro, N. Galletly, F. McCann, B. Treanor, B. Onfelt, D. M. Davis, M. A. A. Neil, and P. M. W. French, "An electronically tunable ultrafast laser source applied to fluorescence imaging and fluorescence lifetime imaging microscopy," *J. Phys. D, Appl. Phys.*, vol. 37, pp. 3296–3303, 2004.

[6] S. Sanders, "Wavelength-agile fiber laser using group-velocity dispersion of pulsed super-continua and application to broadband absorption spectroscopy," *Appl. Phys. B, Lasers Opt.*, vol. 75, pp. 799–802, 2002.

[7] M. Ere-Tassou, C. Przygodzki, E. Fertein, and H. Delbarre, "Femtosecond laser source for real-time atmospheric gas sensing in the UV-visible," *Opt. Commun.*, vol. 220, pp. 215–221, 2003

[8] J. Wegener, R. H. Wilson, and H. S. Tapp, "Mid-infrared spectroscopy for food analysis: Recent new applications and relevant developments in sample presentation methods," *Trends Anal. Chem.*, vol. 18, pp. 85–93, 1999.

[9] A. B. Seddon, "A prospective for new mid-infrared medical endoscopy using chalcogenide glasses," *Int. J. Appl. Glass Sci.*, vol. 2, pp. 177–191, 2011.

[10] J. M. Dudley, G. Genty, and S. Coen, "Supercontinuum generation in photonic crystal fiber," *Rev. Mod. Phys.*, vol. 78, pp. 1135–1184, 2006.

[11] J. Swiderski and M. Michalska, "Mid-infrared supercontinuum generation in a single-mode thulium-doped fiber amplifier," *Laser Phys. Lett.*, vol. 10, p. 035105, 2013.

[12] J. K. Ranka, R. S. Windeler, and A. J. Stentz, "Visible continuum generation in air silica microstructured optical fibers with anomalous dispersion at 800 nm," *Opt. Lett.*, vol. 25, no. 1, pp. 25–27, 2000.

[13] T. S. Saini, A. Baili, V. Dahiya, A. Kumar, R. Cherif, M. Zghal, and R. K. Sinha, "Design of equiangular spiral photonic crystal fiber for supercontinuum generation at 1550 nm," *Proc. SPIE, Photon. Fiber Crystal Devices, Adv. Mater. Innovations Device Appl. VIII*, vol. 9200, pp. 920012-1–920012-6, Sep. 5, 2014.

[14] T. S. Saini, A. Kumar, and R. K. Sinha, "Highly nonlinear triangular core photonic crystal fiber with all normal dispersion for supercontinuum generation," presented at the Frontiers Optics, Tucson, AZ, USA, Oct. 19–23, 2014, Paper FW1D-4.

[15] M. El-Amraoui, G. Gadret, J. C. Jules, J. Fatome, C. Fortier, and J. Troles, "Microstructured chalcogenide optical fibers from As_2S_3 glass: Towards new IR broadband sources," *Opt. Exp.*, vol. 18, pp. 26655–26665, 2010.

[16] L. Liu, G. Qin, Q. Tian, D. Zhao, and W. Qin, "Numerical investigation of mid-infrared supercontinuum generation up to 5 μm in single mode fluoride fiber," *Opt. Exp.*, vol. 19, pp. 10041–10048, 2011.

[17] W. Yuan "2–10 μm mid-infrared supercontinuum generation in As_2Se_3 photonic crystal fiber," *Laser Phys. Lett.*, vol. 10, no. 9, p. 095107, 2013.

[18] P. Yan, R. Dong, G. Zhang, H. Li, S. Ruan, H. Wei, and J. Luo, " Numerical simulation on the coherent time-critical 2–5 μm supercontinuum generation in an As_2S_3 microstructured optical fiber with all-normal flat-top dispersion profile," *Opt. Commun.*, vol. 293, pp. 133–138, 2013.

[19] T. S. Saini, A. Kumar, and R. K. Sinha, "Broadband mid-IR supercontinuum generation in As_2Se_3 based chalcogenide photonic crystal fiber: A new design and analysis," *Opt. Commun.*, vol. 347, pp. 13–19 2015.

[20] V. Shiryaev and M. Churbanov, "Trends and prospects for development of chalcogenide fibers for mid-infrared transmission," *J. Non-Cryst. Solids*, vol. 377, pp. 225–230, 2013.

[21] R. E. Slusher, G. Lenz, J. Hodelin, J. Sanghera, L. B. Shaw, and I. D. Aggarwal, "Large Raman gain and nonlinear phase shift in high-purity As_2Se_3 chalcogenide fibers," *J. Opt. Soc. Am. B*, vol. 21, pp. 1146–1155, 2004.

[22] L. B. Shaw, V. Q. Nguyen, J. S. Sanghera, I. D. Aggarwal, P. A. Thielen, and F. H. Kung, "IR supercontinuum generation in As-Se photonic crystal fiber," presented at the Advanced Solid State Photonics, Vienna, Austria, 2005, Paper TuC5.

[23] J. Hu, C. R. Menyuk, L. B. Shaw, J. S. Sanghera, and I. D. Aggarwal, "Maximizing the bandwidth of supercontinuum generation in As_2Se_3 chalcogenide fibers," *Opt. Exp.*, vol. 18, no. 7, pp. 6722–6739, 2010.

[24] I. Kubat, C. S. Agger, P. M. Moselund, and O. Bang, "Mid-infrared supercontinuum generation to 4.5 μm in uniform and tapered ZBLAN step-index fibers by direct pumping at 1064 or 1550 nm," *J. Opt. Soc. Am. B*, vol. 30, no. 16, pp. 2743–2757, 2013.

[25] M. Klimczak, B. Siwicki, P. Skibinski, D. Pysz, R. Stepien, A. Heidt, C. Radzewicz, and R. Buczynski, "Coherent supercntinuum generation up to 2.3 μm in all-solid soft-glass photonic crystal fibers with flat all-normal dispersion," *Opt. Exp.*, vol. 22, no. 15, pp. 18824–18832, 2014.

[26] I. Kubat, C. R. Petersen, U. V. Moller, A. Seddon, T. Benson, L. Brilland, D. Mechin, P. M. Moselund, and O. Bang, "Thulium pumped mid-infrared 0.9–9 μm supercontinuum generation in concatenated fluoride and chalcogenide glass fibers," *Opt. Exp.*, vol. 22, no. 4, pp. 3959–3969, 2014.

[27] I. Kubat, C. S. Agger, U. Moller, A. B. Seddon, Z. Tang, S. Sujecki, T. M. Benson, D. Furniss, S. Lamrini, K. Scholle, P. Fuhrberg, B. Napier, M. Farries, J. Ward, P. M. Moselund, and O. Bang, "Mid-infrared supercontinuum generation to 12.5μm in large NA chalcogenide step-index fibres pumped at 4.5μm," *Opt. Exp.*, vol. 22, no. 16, pp. 19169–19182, 2014.

[28] C. R. Petersen, U. Moller, I. Kubat, B. Zhou, S. Dupont, J. Ramsay, T. Benson, S. Sujecki, N. Abdel-Moneim, Z. Tang, D. Furniss, A. Seddon, and O. Bang, "Mid-infrared supercontinuum covering the 1.4–13.3 μm molecular fingerprint region using ultra-high NA chalcogenide step-index fibre," *Nature Photon.*, vol. 8, pp. 830–834, Sep. 2014.

[29] G. P. Agrawal, *Nonlinear Fiber Optics*, 5th ed. New York, NY, USA: Elsevier, 2013.

[30] W. Liu, L. Pang, X. Lin, R. Gao, and X. Song, "Observation of soliton fission in microstructured fiber," *Appl. Opt.*, vol. 51, no. 34, pp. 8095–8101, 2012.

[31] A. V. Husakov and J. Herrmann, "Supercontinuum generation of higher order solitons by fission in photonic crystal fibers," *Phys. Rev. Lett.*, vol. 87, p. 203901, 2001.

[32] G. Steinmeyer and J. S. Skibina, "Entering the mid-infrared," *Nature Photon.*, vol. 8, no. 11, pp. 814–815, 2014.

[33] N. Leindecker, A. Marandi, R. L. Byer, K. L. Vodopyanov, J. Jiang, I. Hartl, M. Fermann, and P. Schunemann, "Octave-spanning ultrafast OPO with 2.6–6.1 μm instantaneous bandwidth pumped by femtosecond Tm-fiber laser," *Opt. Exp.*, vol. 20, pp. 7046–7053, 2012.

[34] H. G. Dantanarayana, N. Abdel-Moneim, Z. Tang, L. Sojka, S. Sujecki, D. Furniss, A. B. Seddon, I. Kubat, O. Bang, and T. M. Benson, "Refractive index dispersion of chalcogenide glasses for ultra-high numerical-aperture fiber for mid-infrared supercontinuum generation," *Opt. Mater. Exp.*, vol. 4, no. 7, pp. 1444–1455, 2014.

[35] B. Ung and M. Skorobogatiy, "Chalcogenide microporous fibers for linear and nonlinear applications in the mid-infrared," *Opt. Exp.*, vol. 18, no. 8, pp. 8647–8659, 2010.

[36] B. Hooda and V. Rastogi, "Segmented-core single mode optical fiber with ultra-large-effective-area, low dispersion slop and flattened dispersion for DWDM optical communication systems," *Prog. Electron. Res. B*, vol. 51, pp. 157–175, 2013.

Than Singh Saini was born in 1984 in Aligarh, India. He received the B.Sc. (PCM) and M.Sc. (Physics) degrees from Dr. B. R. A. University, Agra, India, in 2004 and 2006, respectively. He is currently working toward the Ph.D. degree in optics and photonics from Delhi Technological University, Delhi, India. He has published 27 research papers in international journals and conference proceedings. His area of research interest includes specialty optical fibers and waveguides for high-power applications, supercontinuum generation in PCF, and slow-and-fast light generation in PCF. He received three Best Paper Presentation Awards in three international conferences. He is a Student Member of the IEEE, OSA and the SPIE.

Ajeet Kumar was born in 1983 in India. He received the B.Sc. degree from Deen Dayal Upadhayay Gorakhpur University, Gorakhpur, India, in 2002, and the M.Sc. and Ph.D. degrees from the Indian Institute of Technology Roorkee, Roorkee, India, in 2004 and 2009, respectively. He was a Postdoctoral Fellow at the Gwangju Institute of Science and Technology, Korea. In July 2010, he joined the Delhi Technological University, Delhi, India, where he is currently working as an Assistant Professor. He has published more than 70 research articles in journal and conferences. His current research interests include novel large-mode area single-mode fibers, segmented cladding fibers, fiber optic sensors, large-core fiber for solar delivery system, and waveguide long period gratings. He received the Young Scientist Award by Uttarakhand Government, India. He is a Member of the IEEE and OSA.

Ravindra Kumar Sinha received the M.Sc. degree in physics from the Indian Institute of Technology (IIT), Kharagpur, India, in 1984, and the Ph.D. degree in the area of fiber optics and optical communication technology from IIT, Delhi, India, in 1990. He had held various research and academic positions with the Indian Institute of Science, Bangalore, India, during 1991, the Birla Institute of Technology and Science, Pilani, during 1992–1994, REC (now NIT), Hamirpur, during 1994–1998, and has been with the Delhi College of Engineering (now Delhi Technological University—DTU), University of Delhi, Delhi, since 1998. He is currently a Professor of Applied Physics, the Dean (Academic-UG), and the Chief Coordinator of Technology Information, Forecasting and Assessment Council, Centre of Relevance and Excellence in Fiber Optics and Optical Communication at DTU. He has published more than 220 research papers in the leading journals and conference proceedings. He received the Fulbright-Nehru, National Science Council Taiwan, Indo–Swiss Bilateral, Royal Academy of Engineering (U.K.), and the Japan Society for Promotion of Science fellowships and the Japanese Government Scholarship in addition to the assignment of Visiting Scientist at ICTP-Trieste, Italy, IROST (Iran), and University of Campinas, Brazil. He also received the Biman-Behari Sen Memorial Award 2012, the CEOT Optoelectronics Technology Award 2004, and the S. K. Mitra Memorial Award 2002 from the Institution for Electronics and Telecommunication Engineers (IETE), India, for his outstanding research work in the area of photonic crystal fibers and photonic crystal-based nanophotonic devices. He is a Fellow of the International Society for Optical Engineers (SPIE), a Fellow of the IETE, and a Fellow of the Optical Society of India. He has also served numerous administrative responsibilities like the Head of the Department of Applied Physics, the Dean (Industrial Research and Development), and the Chairman of many academic and advisory bodies related to education, research, and product development in the areas of optics and photonics.